Canada, the Natural Sciences and Engineering Research Council of Canada (A5890), and The University of Alberta for generous support. M.J.R. thanks Professor A. D. Broom for facilities and hospitality provided during a visiting professorship at the University of Utah, 1981–82.

Registry No. 1c, 85335-71-3; **1d**, 570-74-1; **1e**, 57-88-5; **2**, 1250-95-9; **2a**, 85354-70-7; **2b**, 20230-22-2; **3**, 582-52-5; **3a**, 19189-62-9; **3b**, 4613-62-1; **4**, 7473-45-2; **4a**, 76700-76-0; **4b**, 76700-79-3; **4e**, 78185-65-6; **5**, 58-61-7; **5a**, 69304-45-6; **5b**, 76700-77-1; **5c**, 84828-84-2; **5d**, 958-09-8; **6**, 118-00-3; **6a**, 69304-44-5; **6b**, 85335-72-4; **6d**, 961-07-9; **7**, 58-96-8; **7a**, 69304-38-7; **7b**, 76700-78-2; **7d**, 951-78-0; **8**, 65-46-3; **8′**, 3768-18-1; **8a′**, 85335-73-5; **8b′**, 85335-74-6; **8c′**, 85335-75-7; **8d**, 951-77-9; **9**, 69-33-0; **9a**, 85335-76-8; **9b**, 85335-77-9; **9c**, 85335-78-0; **9d**, 60129-59-1; **10**, 606-58-6; **10a**, 85335-79-1; **10b**, 85335-80-4; **10c**, 85335-81-5; **10d**, 15676-19-4; **11d**, 83379-28-6; **12**, 5536-17-4; **13a**, 85335-82-6; *ribo*-**14**, 63963-71-3; *arabino*-**14**, 64597-33-7; 1,1,3,3-tetraisopropyldisiloxane, 18043-71-5; trichlorosilane, 10025-78-2; diisopropylsilanol, 18173-84-7; thiophosgene, 463-71-8; phenol, 108-95-2; TPDS-Cl_2, 69304-37-6; PT-C-Cl, 1005-56-7.

Multiple Conformational States of a Pro-Pro Peptide. Solid-State and Solution Conformations of Boc-Aib-Pro-Pro-NHMe

Hemalatha Balaram, B. V. Venkataram Prasad, and P. Balaram*

Contribution from the Molecular Biophysics Unit, Indian Institute of Science, Bangalore 560 012, India. *Received November 2, 1982*

Abstract: The solid-state and solution conformations of the model peptide Boc-Aib-Pro-Pro-NHMe have been studied by X-ray diffraction and NMR. The peptide adopts a poly(proline II) conformation in the solid state. Two molecules are observed in the asymmetric unit differing in the geometry (cis/trans) of the urethane group. The molecules are held together in the crystal by a complex network of hydrogen bonds involving three molecules of water, which cocrystallize. Dissolution of single crystals at low temperature (~233 K) permits NMR observation of the solid-state conformer. In solution, the peptide undergoes a trans-cis isomerization of the Pro–Pro bond. Low-temperature NMR measurements allow the detection of three conformational states of the Pro–Pro segment. Both cis′ and trans′ rotational isomers about the C^{α}–CO (ψ) bond of Pro-3 are detectable at low temperatures. Theoretical calculations suggest an appreciable activation barrier to ψ rotation. Temperature and solvent dependence of NH chemical shifts provide evidence for an intramolecular hydrogen bond, involving the NHMe group in the cis Pro-Pro conformer. Energy calculations suggest the possibility of a type VI β-turn conformation stabilized by a 4 → 1 hydrogen bond between the Aib-1 CO and NHMe groups.

Proline peptides occupy a central position in the development of peptide conformational analysis.[1] The restrictions imposed on the available backbone conformations by the pyrrolidine ring,[2] the possibility of cis–trans isomerism about the X–Pro imide bond,[3] and conformational flexibility of the five-membered ring[4] have all been the focus of several investigations. The extensive occurrence of Pro residues in fibrous protein structures like collagen[5] and tropoelastin[6] has provided a stimulus for these studies. The suggestion that cis–trans isomerization about X–Pro bonds may constitute the rate-determining step in the folding of globular proteins[7] has evoked particular interest in the possibility that Pro residues may modulate the dynamics of polypeptide chain folding.[8] Studies in this laboratory have been directed toward the use of Pro residues in conjunction with stereochemically constrained α-aminoisobutyryl (Aib)[9] residues in developing synthetic model peptides which will exemplify various folded conformations of acyclic peptides.[10] While there exist several examples of 4 → 1 hydrogen-bonded β-turn conformations with all trans peptide backbones,[11] there are, as yet, no examples of a 5 → 1 hydrogen-bonded classical α-helical conformation ($\phi \sim \pm 55°$, $\psi \sim \pm 45°$)[12] in a small acyclic peptide. In an attempt to develop a suitably constrained model, we have examined the peptide Boc-Aib-Pro-Pro-NHMe. The Aib residue is largely restricted to conformations in the helical region ($\phi \pm 60 \pm 20°$, $\psi \sim \pm 30 \pm$

(1) (a) Deber, C. M.; Madison, V.; Blout, E. R. *Acc. Chem. Res.* **1976**, *9*, 106–113. (b) Wyssbrod, H. R.; Gibbons, W. A. *Surv. Prog. Chem.* **1973**, *6*, 207–325. (c) Karle, I. L. "Peptides: Chemistry, Structure and Biology"; Walter, R.; Meienhofer, J., Eds.; Ann Arbor Science Publishers: Ann Arbor, MI, 1975; pp 61–84.

(2) De Tar, D. F.; Luthra, N. *J. Am. Chem. Soc.* **1977**, *99*, 1232–1244.

(3) (a) Deber, C. M.; Bovey, F. A.; Carver, J. P.; Blout, E. R. *J. Am. Chem. Soc.* **1970**, *92*, 6191–6198. (b) Thomas, W. A.; Williams, M. K. *J. Chem. Soc., Chem. Commun.* **1972**, 994. (c) Grathwohl, C.; Wuthrich, K. *Biopolymers* **1976**, *15*, 2025–2041.

(4) (a) Madison, V. *Biopolymers* **1977**, *16*, 2671–2692. (b) London, R. E. *J. Am. Chem. Soc.* **1978**, *100*, 2678–2685. (c) Bach, A. C., II; Bothner-By, A. A.; Gierasch, L. M. *J. Am. Chem. Soc.* **1982**, *104*, 572–576.

(5) Traub, W.; Piez, K. A. *Adv. Protein Chem.* **1971**, *25*, 243–352.

(6) (a) Foster, J. A.; Bruenger, E.; Gray, W. R.; Sandberg, L. B. *J. Biol. Chem.* **1973**, *248*, 2876–2879. (b) Urry, D. W.; Long, M. M. *CRC Crit. Rev. Biochem.* **1976**, *4*, 1–45.

(7) (a) Brandts, J. F.; Halvorson, H. R.; Brennan, M. *Biochemistry* **1975**, *14*, 4953–4963. (b) Brandts, J. F.; Brennan, M.; Lin, L.-N. *Proc. Natl. Acad. Sci. U.S.A.* **1977**, *74*, 4178–4181.

(8) (a) Levitt, M. *J. Mol. Biol.* **1981**, *145*, 251–263. (b) Baldwin, R. L. *Trends Biochem. Sci. (Pers. Ed.)* **1978**, *3*, 66–68.

(9) Abbreviations used: Boc, *tert*-butyloxycarbonyl; DCC, *N,N′*-dicyclohexylcarbodiimide; DMF, *N,N*-dimethylformaide; NHMe, *N*-methylamide.

(10) (a) Venkatachalapathi, Y. V.; Nair, C. M. K.; Vijayan, M.; Balaram, P. *Biopolymers* **1981**, *20*, 1123–1136. (b) Venkatachalapathi, Y. V.; Balaram, P. *Biopolymers* **1981**, *20*, 1137–1145. (c) Venkatachalapathi, Y. V.; Balram, P. *Nature (London)* **1979**, *281*, 83–84. (d) Prasad, B. V. V.; Balaram, H.; Balaram, P. *Biopolymers* **1982**, *21*, 1261–1273. (e) Prasad, B. V. V.; Balaram, P. "Conformation in Biology"; Srinivasan, R.; Sarma, R. H., Ed.: Adenine Press: New York, 1982; pp 133–140.

(11) (a) Smith, J. A.; Pease, L. G. *CRC Crit. Rev. Biochem.* **1980**, *8*, 315–399. (b) Toniolo, C. *CRC Crit. Rev. Biochem.* **1980**, *9*, 1–44. (c) Karle, I. L. "The Peptides"; Gross, E., Meienhofer, J., Eds.; Academic Press: New York, 1981; Vol. 4, pp 1–5.

(12) (a) Ramachandran, G. N.; Sasisekharan, V. *Adv. Protein Chem.* **1968**, *23*, 283–468. (b) IUPAC–IUB Commission on Biochemical Nomenclature *Biochemistry* **1970**, *9*, 3471–3479.

0002-7863/83/1505-4065$01.50/0

20°),[13] while the two L-Pro residues must necessarily have $\phi \sim -60°$. Since Aib-Pro β-turn formation,[10a,14] is precluded by the presence of Pro-3, it was hoped that 5 → 1 hydrogen bonding between the Boc CO and methylamide NH groups may be favored. The results described in this paper establish that in the solid-state Boc-Aib-Pro-Pro-NHMe (**1**) adopts an extended conformation, stabilized by water molecules which serve to cross-link peptide chains by intermolecular hydrogen bonding. Dissolution of single crystals results in a structural transition and as many as three conformations are detectable by low-temperature NMR. Conformational energy calculations provide a framework to rationalize the observed conformational interconversions in solution. Evidence for the occurrence of a Pro-Pro β-turn with a central cis peptide unit is presented. The studies presented below constitute a clear example of extensive differences between the solid-state and solution conformations of a peptide.

Materials and Methods

Synthesis of Boc-Aib-Pro-Pro-NHMe (1). Boc-Aib-Pro-OH[15] (255 mg, 0.86 mmol) was dissolved in DMF (5 mL) and cooled in an ice bath. Pro-OMe (112 mg, 0.86 mmol), 1-hydroxybenzotriazole (116 mg, 0.86 mmol), and DCC (177 mg, 0.86 mmol) were added successively. The reaction mixture was stirred at 0 °C for 4 h and room temperature overnight. The precipitated dicyclohexylurea was filtered off and washed with ethyl acetate. The combined filtrates were washed with H_2O, 1 N HCl, and 1 N Na_2CO_3, dried over Na_2SO_4, and evaporated to yield 217 mg (62%) of Boc-Aib-Pro-Pro-OMe, as an oil. This was used without further purification.

Boc-Aib-Pro-Pro-OMe was dissolved in 20 mL of absolute methanol and the solution saturated with dry methylamine gas. The reaction mixture was tightly stoppered and allowed to stand at room temperature for 24 h. Evaporation of the solvent yielded a solid, which was chromatographed on a silica gel column. The peptide was eluted with 2% CH_3OH–$CHCl_3$: yield 170 mg (75%); mp 106–108 °C. Anal. Calcd for $C_{20}H_{34}N_4O_5$: C, 58.53; N, 13.66; H, 8.29. Found: C, 58.08; N, 13.19; H, 8.68. The peptide was fully characterized by 270-MHz ^1H NMR.

Spectroscopic Studies. The 270-MHz ^1H and 67.89-MHz ^{13}C NMR spectra were recorded on a Bruker WH-270 FT-NMR spectrometer. All chemical shifts are expressed as δ downfield from internal tetramethylsilane. Experimental conditions have been previously described.[16]

X-ray Diffraction. Single crystals of **1** were grown from an ether–methanol solution, containing traces of water. Rotation and Weissenberg photographs indicated an orthorhombic lattice, with space group $P2_12_12_1$, with $a = 8.970$ (1), $b = 17.549$ (3), and $c = 31.152$ (5) Å. The density measured by the flotation method in a CCl_4–benzene mixture was 1.18 g cm^{-3}, yielding a molecular weight of 874, compatible with two molecules of peptide and three water molecules in the asymmetric unit. Intensity data were collected for 4568 unique reflections on a CAD-4 diffractometer by employing an ω-2θ scan, up to a maximum Bragg angle of 65°, using CuKα radiation. Three standard reflections were measured after every 50 reflections, and there was no significant change in the intensities during the period of data collection. The intensities were corrected for Lorentz and polarization factors but not for absorption. All the measured reflections were used for structure determination and refinement.

The structure was solved by using the program MULTAN 80,[17] with some manual intervention. Automatic runs using the convergence mapping procedure of the program invariably led to E maps with one super large peak for most sets, including that with the best figure of merit. The highest combined figure of merit in these runs was 2.2. An inspection of the convergence mapping procedure and the origin defining reflections suggested that the $0kl$ set of reflections bias the E-value distribution. Renormalization of the $0kl$ reflections over the entire data set resulted in a more satisfactory distribution. Several sets of phases were generated with 498 reflections having $E > 1.47$ input into the MULTAN program. An E map with phases obtained from the set of highest combined figure of merit (2.69) revealed 28 atoms of one of the two molecules in the asymmetric unit. Karle recycling[18] yielded all the remaining atoms in the asymmetric unit. Refinement of the positional and isotropic thermal parameters, using a block diagonal least-squares procedure, converged to an R value of 0.24. Difference electron density maps revealed the three water molecules. Further refinement with anisotropic thermal parameter led to an R value of 0.10. Difference electron density maps at this stage revealed 56 hydrogens out of 74. The remaining hydrogens were stereochemically fixed, and subsequent refinement with anisotropic temperature factors for non-hydrogen atoms and isotropic thermal parameters for hydrogens, with a σ-weighting scheme, gave a final R value of 0.062. The positional parameters and isotropic equivalent temperature factors for all the non-hydrogen atoms are given in Table I. Hydrogen atom coordinates and anisotropic temperature factors are provided as supplementary material (see paragraph at end of paper regarding supplementary material).

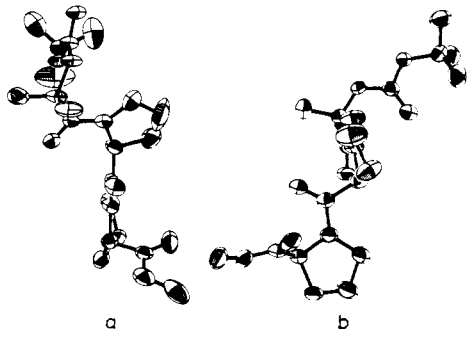

Figure 1. Perspective view of the molecular conformation of Boc-Aib-Pro-Pro-NHMe, **1**, in the crystalline state: (a) molecule A; (b) molecule B.

Conformational Energy Calculations. Theoretical energy calculations using semiempirical methods have been carried out on the model compounds Ac-Pro-Pro-NHMe and Ac-Aib-Pro-Pro-NHMe. The general methodology for the computation of conformational energies of Pro peptides has been described earlier.[19] In Ac-Pro-Pro-NHMe $\phi_{Pro\text{-}1}$ and $\phi_{Pro\text{-}2}$ are restricted to approximately −60°. For energy calculations ψ's have been varied from −180° to 180° at 10° intervals, while ϕ's have been restricted to the region −50° to −80°. Six states of puckering have been considered which span the region of chosen ϕ values. These are A_1, A_2, and A_3 conformations corresponding to ϕ = −50°, −60°, and −70°, respectively, in the C^γ-exo type and B_2, B_3, and B_4 corresponding to ϕ = −60°, −70°, and −80°, respectively, in the C^γ-endo type.[20] The rationale for this choice has been described earlier.[19] For each pair of $\phi_{Pro\text{-}1}$ and $\phi_{Pro\text{-}2}$, ψ_1, ψ_2 plots have been constructed, leading to 36 ψ_1, ψ_2 energy maps considering cis and trans-Pro-Pro conformers with the various Pro puckered states. The geometries used for the trans and cis Pro-Pro peptide units are the same. Figure 9 shows the energetically most favorable situation. In the case of Ac-Aib-Pro-Pro-NHMe ϕ, ψ of Aib was varied from −100° to 0° in the right-handed helical region and 0° to 100° in the left-handed helical region.[13] The Pro-Pro cis conformer was chosen for energy calculations. Conformational energies were computed only for structures having a stereochemically satisfactory hydrogen bond, with the N---O distance between 2.8 and 3.2 Å and ∠H-N-O < 35°.

Results and Discussion

Molecular Conformation in the Solid State. Figure 1 shows a perspective view of the conformations of the two independent molecules in the asymmetric unit of the crystals of **1**. The bond lengths and valence angles are given in Figures 2 and 3. The relevant backbone and pyrrolidine ring torsion angles[12] are summarized in Table II. There are no intramolecular hydrogen bonds

(13) (a) Nagaraj, R.; Balaram, P. *Acc. Chem. Res.* **1981**, *14*, 356–362. (b) Marshall, G. R.; Bosshard, H. E. *Circ. Res., Suppl. 2* **1972**, *30/31*, 143–150. (c) Toniolo, C.; Bonora, G. M.; Bavoso, A.; Benedetti, E.; DiBlasio, B.; Pavone, V.; Pedone, C. *Biopolymers* **1983**, in press. (d) Benedetti, E.; Bavoso, A.; DiBlasio, B.; Pavone, V.; Pedone, C.; Crisma, M.; Bonora, G. M.; Toniolo, C. *J. Am. Chem. Soc.* **1982**, *104*, 2437–2444. (e) Butters, T.; Hutter, P.; Jung, G.; Pauls, N., Schmitt, H.; Sheldrick, G. M.; Winter, W. *Angew. Chem., Int. Ed. Engl.* **1981**, *20*, 889–890.

(14) (a) Nagaraj, R.; Shamala, N.; Balaram, P. *J. Am. Chem. Soc.* **1979**, *101*, 16–20. (b) Prasad, B. V. V.; Shamala, N.; Nagaraj, R.; Chandrasekaran, R.; Balaram, P. *Biopolymers* **1979**, *18*, 1635–1646. (c) Rao, Ch. P.; Balaram, P. *Biopolymers* **1982**, *21*, 2461–2472.

(15) Iqbal, M. Ph.D. Thesis, Indian Institute of Science, Bangalore, 1982.

(16) Nagaraj, R.; Balaram, P. *Biochemistry* **1981**, *20*, 2828–2835.

(17) Main, P.; Fiske, S. J.; Hull, S. E.; Lessinger, L.; Germain, G.; Declercq, J. P.; Woolfson, M. M. "MULTAN 80, a System of Computer Programs for the Automatic Solution of Crystal Structures from X-ray Diffraction Data"; University of York: York, England, 1980.

(18) Karle, J. *Acta Crystallogr., Sect. B* **1968**, *B24*, 182–186.

(19) Prasad, B. V. V.; Balaram, P. *Int. J. Biol. Macromol.* **1982**, *4*, 99–102.

(20) Ramachandran, G. N.; Lakshminarayanan, A. V.; Balasubramanian, R.; Tegoni, G. *Biochim. Biophys. Acta* **1970**, *221*, 165–181.

Table I. Fractional Coordinates (×10⁴) and Isotropic Equivalent Temperature Factors (Å²) for Non-Hydrogen Atoms in the Asymmetric Unit[a]

	molecule A				molecule B			
atom	*x*	*y*	*z*	B_{eq}	*x*	*y*	*z*	B_{eq}
C_{B_1}	7225 (6)	−1086 (2)	5284 (1)	3.60	11591 (4)	−2397 (2)	6307 (1)	3.16
C_{B_2}	8471 (7)	−1653 (3)	5272 (2)	5.30	11592 (6)	−11569 (3)	6449 (2)	4.84
C_{B_3}	5786 (7)	−1451 (4)	5146 (2)	6.46	12262 (6)	−2854 (3)	6657 (2)	4.80
C_{B_4}	7582 (13)	−409 (3)	5019 (2)	8.73	12378 (5)	−2477 (3)	5883 (2)	4.07
O_1^1	7104 (4)	−766 (1)	5717 (1)	3.63	10002 (3)	−2562 (1)	6260 (1)	3.05
C_1	6627 (4)	−1164 (2)	6052 (1)	2.50	9525 (4)	−3280 (2)	6152 (1)	2.87
O_1^2	6330 (3)	−1849 (1)	6044 (1)	3.04	10337 (3)	−3826 (1)	6110 (1)	3.70
N_2	6429 (4)	−734 (2)	6400 (1)	2.69	8047 (3)	−3278 (2)	6123 (1)	2.98
C_2^{α}	7004 (5)	54 (2)	6459 (1)	2.90	7234 (4)	−3977 (2)	6000 (1)	2.98
$C_2^{\beta_1}$	8702 (6)	54 (2)	6460 (1)	4.10	5558 (5)	−3817 (3)	6025 (2)	4.47
$C_2^{\beta_2}$	6350 (7)	333 (2)	6888 (1)	4.42	7606 (6)	−4216 (3)	5540 (1)	4.14
C_2	6461 (4)	614 (2)	6108 (1)	2.61	7548 (4)	−4640 (2)	6308 (1)	2.72
O_2	7350 (3)	1080 (1)	5966 (1)	5.32	7613 (3)	−5294 (1)	6160 (1)	3.35
N_3	5048 (4)	623 (2)	5978 (1)	3.08	7674 (4)	−4539 (2)	6735 (1)	2.94
C_3^{δ}	3769 (6)	144 (3)	6102 (2)	4.76	7541 (6)	−3842 (2)	6996 (1)	4.21
C_3^{γ}	2555 (6)	466 (4)	5846 (3)	8.54	7316 (9)	−4137 (3)	7438 (2)	6.21
C_3^{β}	3017 (6)	1000 (3)	5524 (2)	5.23	8106 (7)	−4900 (3)	7454 (2)	4.95
C_3^{α}	4636 (5)	1207 (2)	5657 (1)	3.08	7856 (5)	−5222 (2)	7002 (1)	3.23
C_3	4633 (4)	2000 (2)	5872 (1)	2.65	6422 (4)	−5692 (2)	6984 (1)	2.63
O_3	4443 (3)	2079 (2)	6261 (1)	3.26	5207 (3)	−5419 (1)	6915 (1)	3.35
N_4	4785 (4)	2589 (2)	5606 (1)	2.54	6584 (4)	−6446 (2)	7060 (1)	2.59
C_4^{δ}	4917 (5)	2561 (3)	5137 (1)	3.56	7990 (5)	−6862 (2)	7138 (2)	3.99
C_4^{γ}	4598 (5)	3405 (2)	5006 (1)	3.65	7498 (6)	−7686 (2)	7057 (2)	4.52
C_4^{β}	5231	3844 (2)	5382 (1)	3.57	5935 (5)	−7712 (2)	7220 (1)	3.25
C_4^{α}	4766 (4)	3370 (2)	5776 (1)	2.63	5625 (4)	−6926 (2)	7119 (1)	2.34
C_4	3214 (4)	3602 (2)	5919 (1)	2.87	4238 (5)	−6682 (2)	7479 (1)	2.60
O_4	2105 (3)	3387 (2)	5726 (1)	4.03	4725 (3)	−6385 (2)	7809 (1)	3.32
N_5	3168 (4)	4091 (2)	6249 (1)	3.66	2833 (4)	−6882 (2)	7423 (1)	3.10
C_5^{α}	1758 (7)	4377 (3)	6423 (2)	5.39	1711 (5)	−6788 (3)	7753 (2)	4.18
W_1	1748 (5)	2226 (2)	6718 (1)	4.77				
W_2	−496 (4)	2190 (2)	5640 (1)	6.57				
W_3	−915 (5)	3635 (3)	6119 (1)	6.96				

[a] esd's are given in parentheses.

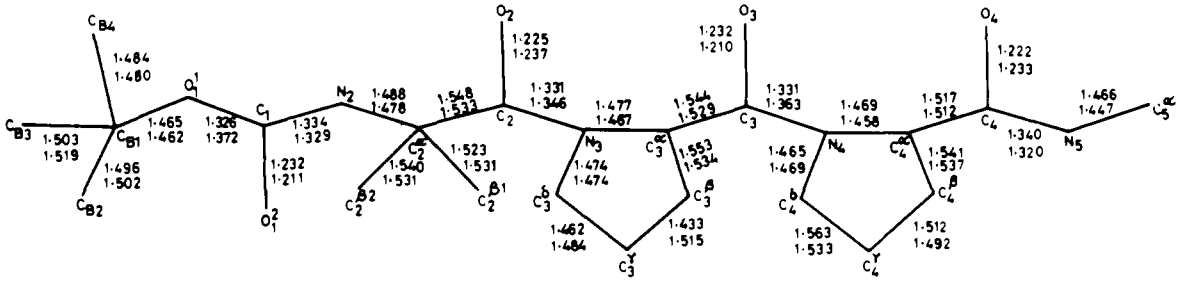

Figure 2. Bond lengths in angstroms in **1**. Numbers on the top are for molecule A and lower numbers for molecule B.

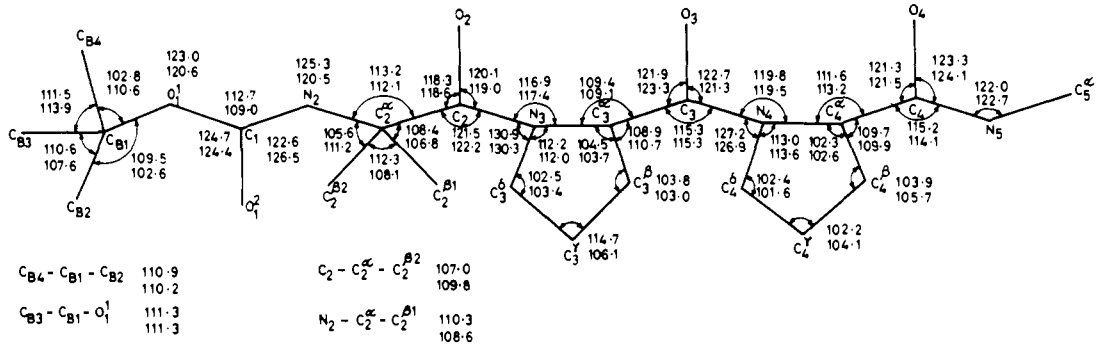

Figure 3. Bond angles in degrees. Numbers on the top are for molecule A and lower numbers for molecule B.

in the structure. An interesting feature is the occurrence of both cis and trans geometries of the urethane protecting group. In studies of Boc-protected peptides cis geometries have generally been observed for Pro residues.[2,21] A few examples of cis urethane groups have also been reported in the cases of protected amino acids.[22] While crystal structures of several peptides with the Boc-Aib group have been solved,[23] the present example is the first

(21) Benedetti, E.; Pedone, C.; Toniolo, C.; Nemethy, G.; Pottle, M. S.; Scheraga, H. A. *Int. J. Pept. Protein Res.* **1980**, *16*, 156–172.

(22) (a) Bats, J. W.; Fuess, H.; Kessler, H.; Schuck, R. *Chem. Ber.* **1980**, *113*, 520–530. (b) Benedetti, E.; DiBlasio, B.; Pavone, V.; Toniolo, C.; Bonora, G. M. *Biopolymers* **1981**, *20*, 1635–1650.

Table II. Backbone and Pyrrolidine Ring Conformational Angles (Degrees)

	ϕ	ψ	ω	θ	χ_1	χ_2	χ_3	χ_4
molecule A								
Aib	57.5 (5)	44.2 (5)	176.9 (3)					
Pro	−71.3 (4)	158.1 (3)	178.7 (3)	−8.3 (4)	13.7 (5)	−15.5 (7)	10.5 (7)	0.5 (5)
Pro	−71.8 (4)	148.6 (3)	179.5 (4)	−11.6 (4)	32.4 (4)	−40.5 (4)	−32.7 (4)	−13.1 (4)
molecule B								
Aib	58.3 (4)	39.1 (5)	175.2 (3)					
Pro	−67.0 (4)	157.1 (3)	173.2 (3)	−9.6 (4)	26.7 (5)	−35.1 (6)	29.1 (5)	−11.9 (5)
Pro	−62.3 (4)	154.4 (3)	172.1 (3)	1.2 (4)	−22.5 (4)	34.8 (4)	−32.7 (4)	19.6 (4)

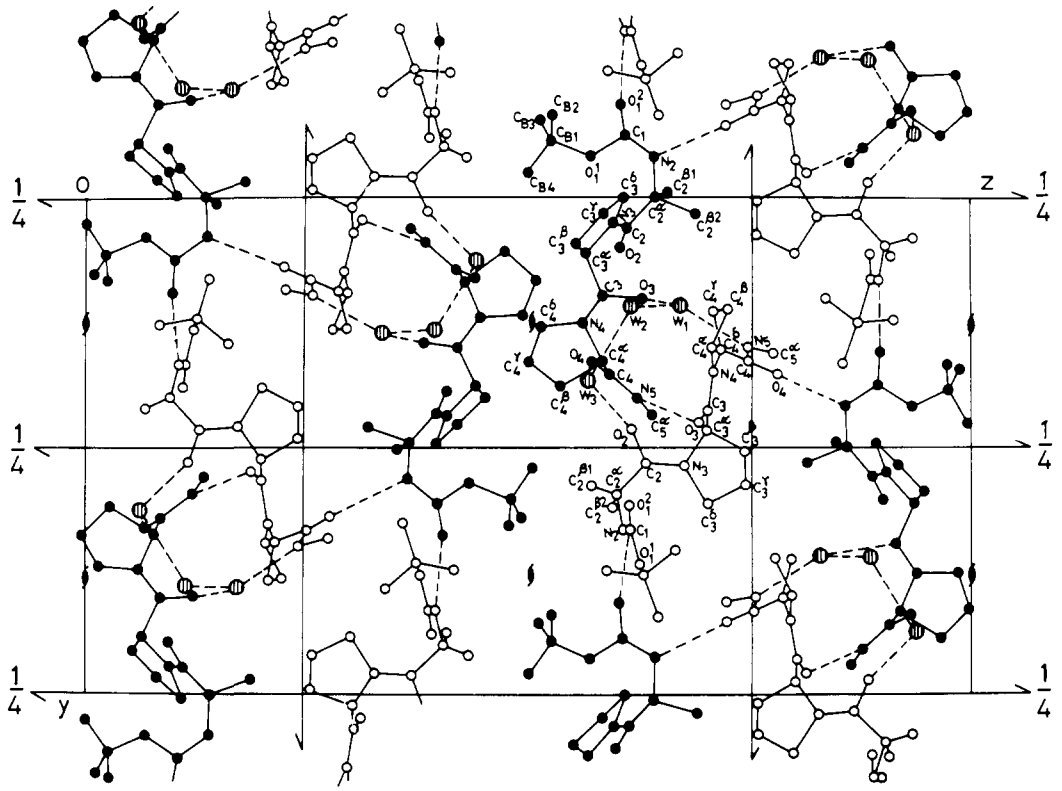

Figure 4. Molecular packing in the crystal structure, viewed down the *a* axis. Molecule A and its symmetry-related neighbors are shown by closed circles, while open circles represent molecule B. W_1, W_2, and W_3 are the three water oxygen atoms. Hydrogen bonds are indicated by dashed lines.

observation of a cis urethane conformation for this moiety.

In both molecules A and B the peptide units are all trans, with the Pro-Pro segment adopting a poly(Pro II) conformation ($\phi \sim -70°$, $\psi \sim 150°$). The tendency of Pro residues to favor these conformations in oligoproline peptides has been established earlier.[24] A similar conformation has also been noted in segments of cytochrome *c* and pancreatic trypsin inhibitor which contain contiguous Pro residues.[25] The ring conformations observed in the crystal structure of **1** are $C^{\gamma}_{endo} - C^{\gamma}_{endo}$ in molecule A and $C^{\gamma}_{endo} - C^{\gamma}_{exo}$ in molecule B.[26] Thus, varied Pro ring conformations can be accommodated in the poly(Pro II) structure. An abnormally short $C^{\beta}_3 - C^{\gamma}_3$ distance of 1.433 Å and an unusually large $C^{\delta}_3 - C^{\gamma}_3 - C^{\beta}_3$ angle of 114.7° is observed for the Pro-2 residue in molecule A. These deviations must be associated with the large B_{eq} of 8.5 Å^2 for the C^{γ}_3 atom.

Several crystal structure determinations of Aib peptides have provided examples of the occurrence of these residues in the right (negative ϕ, ψ) or left (positive ϕ, ψ) handed helical regions of conformational space.[13] In oligopeptides which contain L-amino acids in addition to Aib, right-handed helical structures are invariably favored. Carboxyl-terminal Aib residues in right-handed helical oligopeptides frequently favor ϕ, ψ values in the *left*-handed helical region.[27] The structure of **1** is an intriguing example of

Table III. Hydrogen-Bond Parameters

donor A-H	acceptor B	A···B (Å)	H···B (Å)	HA···B (deg)
W_1-H_2	O_3 (A)	2.817	1.976	15.6
W_1-H_1	W_2	2.745	2.036	10.2
N_5-H_5 (B)	W_1	2.867	2.021	9.0
	$(x, 1 + y, z)$			
W_2-H_1[a]	O_2 (A)	2.785		
	$(x - 1, y, z)$			
W_2-H_2[a]	W_3	2.966		
W_3-H_2	O_2 (B)	2.810	2.130	20.3
	$(x - 1, 1 + y, z)$			
W_3-H_1[a]	O_4 (A)	2.757		
N_2-H_2 (B)	O^2_1 (A)	2.953	1.999	14.3
N_5-H_5 (A)	O_3 (B)	2.896	2.117	19.2
	$(x, 1 + y, z)$			
N_2-H_2 (A)	O_4 (B)	2.904	2.031	2.3
	$(1 - x, 1/2 + y, 3/2 + z)$			

[a] These hydrogen atoms could not be located in the difference Fourier maps.

(23) (a) See ref 13c for a listing of several structures. (b) Prasad, B. V. V.; Sudha, T. S.; Balaram, P. *J. Chem. Soc., Perkin Trans. 1* **1983**, 417–421.
(24) (a) Matsuzaki, T. *Acta Crystallogr., Sect. B* **1974**, *B30*, 1029–1036. (b) Kartha, G.; Ashida, T.; Kakudo, M. *Acta Crystallogr., Sect. B* **1974**, *B30*, 1861–1866. (c) Tanaka, I.; Ashida, T.; Shimonishi, Y.; Kakudo, M. *Acta Crystallogr., Sect. B* **1979**, *B35*, 110–114.
(25) (a) Almassy, R. J.; Dickerson, R. E. *Proc. Natl. Acad. Sci. U.S.A.* **1978**, *75*, 2674–2678. (b) Huber, R.; Kukla, D.; Ruhlmann, A.; Steigemann, W. *Cold Spring Harbor. Symp. Quant. Biol.* **1971**, *36*, 141–148.
(26) Ashida, T.; Kakudo, M. *Bull. Chem. Soc. Jpn.* **1974**, *47*, 1129–1133.

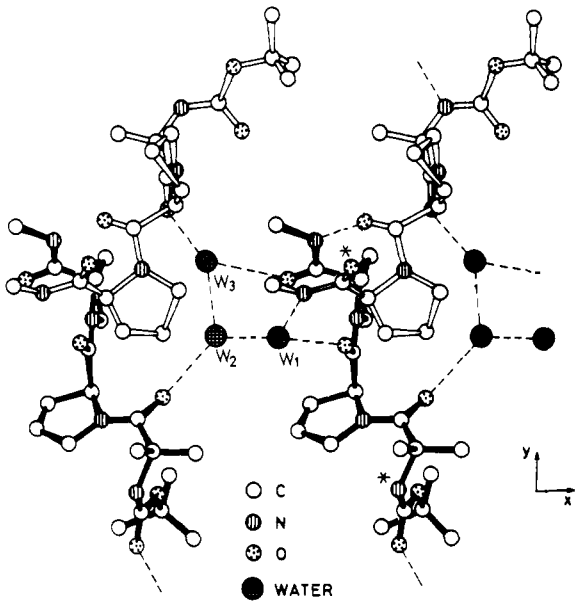

Figure 5. A view of the crystal down the *c* axis illustrating peptide–peptide, peptide–water, and water–water hydrogen bonding. Dark bonds represent molecule A and open bonds represent molecule B. W_1, W_2, and W_3 are the water oxygen atoms. N_2 of A and O_4 of B (starred atoms) are hydrogen bonded to symmetry related molecules.

an amino-terminal Aib residue in a nonhelical peptide, adopting positive, ϕ, ψ values.

Molecular Packing in Crystals of 1. The crystal structure is stabilized by a complex network of intermolecular hydrogen bonds involving the peptide and three water molecules. The various hydrogen bond parameters are listed in Table III. Figure 4 provides a view of the molecular packing. Molecules A and B in the asymmetric unit are arranged in head to head fashion, linked through a hydrogen bond involving adjacent Boc CO and NH groups. The A–B units are placed in columns with the C-terminal ends of neighboring units being linked via two water molecules. Columns in the crystal which are related by the 2_1 screw axis are held together by an intermolecular hydrogen bond between N_2H_2 of molecule A and C_4O_4 of molecule B. Adjacent columns which are related by translational symmetry (along the shortest axis of the crystal) are cemented by involvement of all three water molecules. This is clearly illustrated in a view of the crystal structure down the *Z* axis (Figure 5). This structure is an illuminating example of the role of water molecules in promoting peptide association and may be of value in assessing models of poly-Pro[28] and collagen,[29] which incorporate water.

Conformational Transitions on Dissolution of Crystals. Figure 6a shows the 270-MHz ^{1}H NMR spectrum of a *noncrystalline* sample of **1** in $CDCl_3$ at 233 K. Three distinct conformational states are observed at this temperature as established by the appearance of three sets of methylamide NH (δ 7.14, 8.24, 8.29) and NCH_3 (δ 2.76, 2.81, 2.76) resonances. In order to characterize the NMR spectrum of the conformation observed in the solid state, a spectrum of **1** was recorded at ~233 K, immediately after dissolution of *single crystals* in precooled $CDCl_3$ (Figure 6b). Only a single conformer (I) is detectable, which may be assigned to the poly(Pro II) type structure observed in the crystalline solid. The inset of Figure 6 shows the NCH_3 resonance as a function of temperature. When the sample was warmed, two additional doublets become apparent, indicating the population of additional conformational states (II and III). At ~293 K the doublets due to II and III coalesce and at higher temperatures only two sharp doublets are seen. Thus, a relatively facile exchange process permits interconversion of conformers II and III, while a larger activation barrier separates I from the other two states. The room temperature spectra obtained from the crystalline and noncrystalline samples were identical, indicative of an equilibrium distribution of conformers.

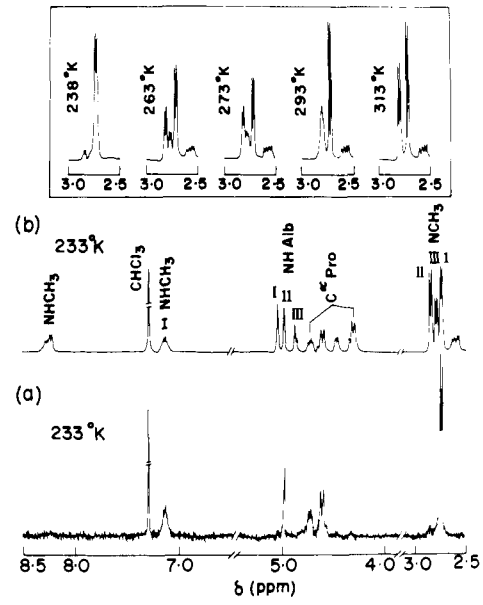

Figure 6. (a) Low-temperature 270-MHz ^{1}H NMR spectrum of single crystals of **1** recorded immediately after dissolution in $CDCl_3$, precooled in liquid N_2, and transferred to the probe at 233 K. (b) Low-temperature 270-MHz ^{1}H NMR spectrum of a *noncrystalline* sample of **1**. (Inset) *N*-methyl resonances (doublets) of the methylamide group in **1**. The sample was prepared as in (a) and the spectra were recorded at various temperatures.

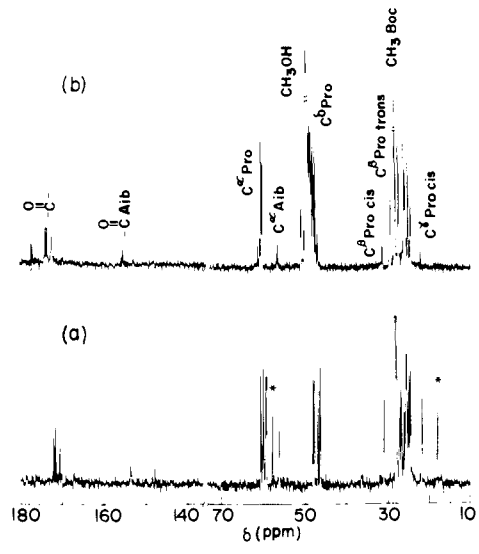

Figure 7. 67.89-MHz ^{13}C NMR spectra of **1** (noncrystalline) in (a) $CDCl_3$ and (b) CH_3OH–$CDCl_3$ (3:1). Starred resonances correspond to ethanol.

(27) (a) The ϕ, ψ values for the C-terminal residues are positive in the following right-handed helical peptides: Z-Aib-Pro-Aib-Ala-OMe,[14a] Boc-Ala-Aib-Ala-Aib-Aib-OMe,[27b] Boc-Leu-Aib-Pro-Val-Aib-OMe,[14c] Boc-Pro-Aib-Ala-Aib-OBz.[27c] In the achiral peptides tosyl-$(Aib)_5$-OMe[27d] and Z-$(Aib)_5$-OBu^t[13d] the ϕ, ψ values of Aib-5 are opposite in sign to the other four residues, the centrosymmetric crystals containing enantiomeric helices. (b) Francis, A. K.; Rao, Ch. P.; Iqbal, M.; Nagaraj, R.; Vijayan, M.; Balaram, P. *Biochem. Biophys. Res. Commun.* 1982, *106*, 1240–1247. (c) Smith, G. D.; Pletnev, V. Z.; Duax, W. L.; Balasubramanian, T. M.; Bosshard, H. E.; Czerwinski, E. W.; Kendrick, N. C. E.; Mathews, F. S.; Marshall, G. R. *J. Am. Chem. Soc.* 1981, *103*, 1493–1501. (d) Shamala, N.; Nagaraj, R.; Balaram, P. *J. Chem. Soc., Chem. Commun.* **1978**, 996–997.

(28) Krimm, S.; Venkatachalam, C. M. *Proc. Natl. Acad. Sci. U.S.A.* **1971**, *68*, 2468–2471.

(29) Suzuki, E.; Fraser, R. D. B.; MacRae, T. P. *Int. J. Biol. Macromol.* **1980**, *2*, 54–56.

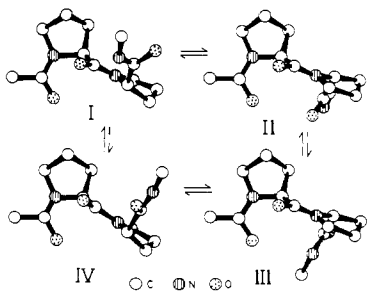

Figure 8. Perspective views of the low-energy conformations of a Pro-Pro sequence. Calculations were performed on the model Ac-Pro-Pro-NHMe. I (trans–trans′); II (cis–trans′); III (cis–cis′); IV (trans–cis′). Regions corresponding to these are shown in Figure 9.

corresponding to cis X-Pro conformers.[30] Since population of cis isomers about the Aib–Pro bond is extremely unfavorable, the assignment of these resonances to cis Pro-Pro conformers is unambiguous. The population of cis conformers in $CHCl_3$ is 45% and is dramatically reduced to 24% in CH_3OH–$CHCl_3$ (3:1). A comparison of the relative peak intensities in the ^{13}C and ^1H spectra, together with the X-ray structuure determination, allows assignment of the trans Pro-Pro structure to I and the cis geometry to II and III.

In L-Pro peptides ϕ_{Pro} is restricted by ring formation to approximately $-60 \pm 15°$. Two distinct regions of conformational space corresponding to different ψ_{Pro} values are energetically favored. These are the cis′ ($\psi \sim -50°$, α-helical region) and trans′ [$\psi \sim 130°$, poly(Pro II) region] conformers. An energy minimum is also encountered at $\psi \sim 70°$, corresponding to the γ-turn or C_7 structure.[4a] Relatively high activation barriers may be encountered for rotation about the C^α–CO (ψ) bond, a process interconverting the cis′ and trans′ conformers. Experimental estimates of $\Delta G^\ddagger$ have yielded values of ~ 14 kcal mol^{-1} in the cyclic peptide, c(Gly-Pro)$_2$[31] and the acyclic derivative Z-Pro-NHMe.[32] The observation of two distinct conformers (II and III) in the cis Pro-Pro state of **1** may be attributed to restricted rotation at low temperature about either Pro-2 or Pro-3 C^α–CO (ψ) bonds. Inspection of molecular models suggests that trans′ geometries are sterically suitable for Pro-2 ψ, while unfavorable interatomic contacts are encountered in the cis′ structure. In contrast, both cis′ and trans′ states are easily accessible for the terminal residue, Pro-3. It is thus reasonable to infer that conformers II and III correspond to Pro-3 trans′ and cis′ states (Figure 8). Further support for this interpretation is obtained from conformational energy calculations on the model fragment Ac-Pro-Pro-NHMe (see Materials and Methods for details).

Theoretical Conformational Analysis. Figure 9 shows conformational energy maps obtained by variations of $\psi_{Pro\text{-}1}$ and $\psi_{Pro\text{-}2}$ in Ac-Pro-Pro-NHMe for both trans ($\omega = 180°$) and cis ($\omega = 0°$) geometries of the Pro–Pro bond. Such ψ_1, ψ_2 maps were examined for various combinations of Pro ring puckering. Only the plots for the B_3, B_3 states (see Materials and Methods), which are energetically the most favorable, are shown in Figure 9, in the region $\psi = 100$–$180°$ for both cis and trans Pro-Pro isomers. For $\psi_1 \sim -40°$ (cis′) favorable conformations are found over a very limited region of ψ_1, ψ_2 space: only for the A_1, A_3 combination of pyrrolidine ring puckering, in the case of the trans Pro-Pro structure. There are no low-energy conformations in this region for the cis Pro-Pro conformer and hence they are not shown in Figure 9b. The results suggest that for trans Pro-Pro structures ψ_1 is preferentially restricted to the trans′ region ($\psi_1 \sim 130$–$160°$), while for ψ_2, population of both cis′ and trans′ regions is possible. In the cis Pro-Pro structure, the allowed regions for ψ_1 and ψ_2 are similar but considerably reduced. The perspective structures of the low-energy conformational states of the Pro-Pro sequence are illustrated in Figure 8. Figure 9c shows a comparison of the energies computed for varying values of ψ_2 for a fixed ψ_1 value of $\sim 160°$ (trans′). It is clear that the barrier to ψ_2 rotation in the trans Pro-Pro case is much less than in the cis Pro-Pro structure. While these calculations do not yield absolute values of activation barriers, a comparison between two similar cases is certainly reasonable. The results of the above calculations suggest that in solution the ^1H NMR spectrum, at the lowest temperatures studied (~ 233 K), for the trans Pro-Pro conformer I may be dynamically averaged over the trans′ (I) and cis′ (IV) structures for the C-terminal Pro residue. The larger activation barriers in the cis Pro-Pro structure permits a freezing out of the two rotational isomers (II and III, Figure 8) about the C-terminal C^α–CO (ψ) bond in **1**.

Solution Conformations of Boc-Aib-Pro-Pro-NHMe. The equilibrium distribution of the various conformations of **1** varies markedly with the nature of the solvent. While cis Pro-Pro conformers are highly populated in non-hydrogen bonding solvents like $CDCl_3$ (45% cis, 55% trans), there is a dramatic increase in the population of Pro-Pro trans structures in solvents like CH_3OH (75%) or $(CD_3)_2SO$ (90%). An examination of Boc-Aib-Pro-Pro-OMe in these solvents revealed that the trans Pro-Pro conformer is overwhelmingly predominant (>95%) even in $CDCl_3$. Thus, introduction of the C-terminal methylamide group stabilizes the Pro-Pro cis geometry. In order to establish whether the methylamide NH group is involved in hydrogen bonding, temperature[33] and solvent dependences[34] of NH chemical shifts were studied. The temperature coefficient values [$d\delta/dT$ (ppm/°C)] for the NH resonances are as follows: for Aib NH (trans Pro-Pro), 0.008; for NHMe (trans), 0.005; for NHMe(cis), 0.002. The Aib NH resonance of the cis Pro-Pro conformer was broadened considerably at higher temperatures. The solvent dependence of NH chemical shifts in $CDCl_3$–$(CD_3)_2SO$ mixtures of varying composition are shown in Figure 10. The Aib NH peaks of both conformers and the NHMe resonance of the trans Pro-Pro conformer show large downfield shifts with increasing concentration of $(CD_3)_2SO$, a strongly hydrogen bonding solvent. In contrast, the NHMe resonance of the cis Pro-Pro conformer is affected to a much smaller extent, suggesting that it may be shielded from the solvent. This resonance also has a very low $d\delta/dT$ value, characteristic of a solvent-shielded hydrogen, whereas all the other resonances have $d\delta/dT > 0.005$ ppm/°C, suggestive of their exposure to solvent.[33] These results establish the absence of any intramolecular hydrogen bonds in the all-trans conformer in solution, in agreement with the X-ray crystal structure determination. However, in the cis Pro-Pro conformer the methylamide NH group appears to be involved in an intramolecular hydrogen bond. Steric shielding of this terminal group is unlikely.

Three conformational possibilities must be considered, depending upon the C=O group involved in hydrogen bonding. These are the $5 \rightarrow 1$ (Boc CO, C_{13}), $4 \rightarrow 1$ (Aib-1 CO, C_{10}), and $3 \rightarrow 1$ (Pro-2 CO, C_7) hydrogen bonds.[11] For a cis Pro-Pro geometry, computer model building clearly rules out the $5 \rightarrow 1$ and $3 \rightarrow 1$ structures. A conformational energy calculation (see Materials and Methods) shows that a good $4 \rightarrow 1$ hydrogen bond is possible in the region described by conformer III, in Figure 9b. This is similar to the molecular perspective shown in Figure 8. The conformational parameters for the lowest energy structure incorporating a stereochemically satisfactory $4 \rightarrow 1$ hydrogen bond are

$\phi_{Pro\text{-}1} = -50°$ $\quad \psi_{Pro\text{-}1} = 160°$ $\quad \phi_{Pro\text{-}2} = -80°$

$\psi_{Pro\text{-}2} = 10°$ $\quad \angle H\text{-}N\text{-}O = 32.9°$ $\quad N\cdots O = 3.03$ Å

This structure corresponds approximately to a type VI β-turn.[10,35] Crystal structure observations of a $4 \rightarrow 1$ hydrogen bond, with

(30) Wuthrich, K. "NMR in Biological Research: Peptides and Proteins"; North-Holland, Amsterdam, 1976.
(31) Deber, C. M.; Fossel, E. T.; Blout, E. R. *J. Am. Chem. Soc.* **1974**, *96*, 4015–4017.
(32) Nagaraj, R.; Venkatachalapathi, Y. V.; Balaram, P. *Int. J. Pept. Protein Res.* **1980**, *16*, 291–298.
(33) Kopple, K. D.; Ohnishi, M.; Go, A. *J. Am. Chem. Soc.* **1969**, *91*, 4264–4272.
(34) Pitner, T. P.; Urry, D. W. *J. Am. Chem. Soc.* **1972**, *94*, 1399–1400.
(35) Lewis, P. N.; Momany, F. A.; Scheraga, H. A. *Biochim. Biophys. Acta* **1973**, *303*, 211–229.

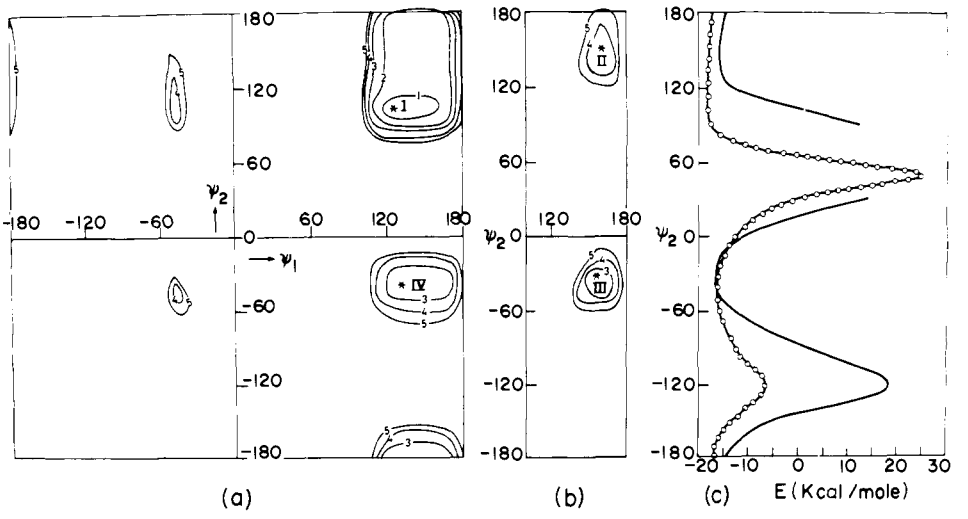

Figure 9. ψ_1, ψ_2 conformational energy maps for Pro-Pro sequences: (a) trans Pro-Pro; (b) cis Pro-Pro. Energy contours are drawn at a 1 kcal mol^{-1} interval from the minumum energy. I–IV represent the conformations depicted in Figure 8. (c) Variation of conformational energy with ψ_2 in Ac-Pro-Pro-NHMe, with ψ_1 fixed at 160°. (O) trans Pro-Pro; (—) cis Pro-Pro.

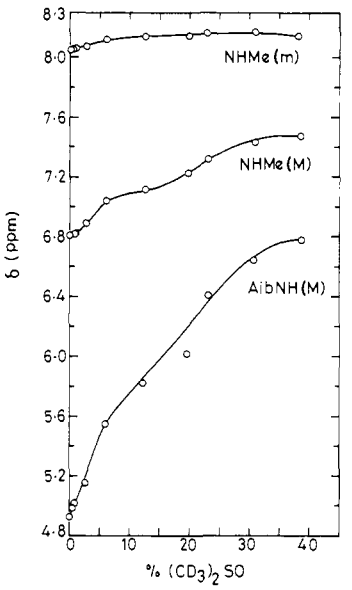

Figure 10. Solvent dependence of NH chemical stiffs in **1** in $CDCl_3$–$(CD_3)_2SO$ mixtures of varying composition.

a central cis peptide unit, have been reported in peptides with N-alkylated amino acids at the $i + 2$ position of the β-turn.[36] The NMR studies described above have been carried out in $(CD_3)_2SO$ and $CDCl_3$–$(CD_3)_2SO$ mixtures. It should be noted that there is a large decrease in the population of cis Pro-Pro conformers on addition of $(CD_3)_2SO$ to $CDCl_3$. The type VI β-turn structure is therefore more favored in media of low hydrogen bonding ability.

Conclusions

Studies in the solid state and in solution of the model peptide Boc-Aib-Pro-Pro-NHMe have provided experimental evidence for the population of multiple conformational states in acyclic Pro-Pro peptides. The crystal structure provides an example of the role of bridging water molecules in stabilizing all-trans poly(Pro II) conformations. Dissolution of single crystals at low temperatures (~233 K) permits ^1H NMR observation of the all-trans conformer, while warming allows detection of two additional conformational states corresponding to the cis Pro-Pro conformer, differing in their values of $\psi_{Pro\text{-}3}$. Conformational energy calculations provide a rationalization of these observations. Larger activation barriers to $\psi_{Pro\text{-}3}$ rotation are envisaged in the cis Pro-Pro conformer as compared to the trans Pro-Pro structure. ^1H NMR studies of the equilibrium conformational distribution suggest that in the cis Pro-Pro conformer, there is a significant population of states in which the methylamide NH is hydrogen bonded. Model building and energy calculations support a type VI β-turn in the cis Pro-Pro conformer, while NMR results indicate that this conformation is stabilized in solvents of low hydrogen bonding ability. The results of this investigation provide evidence for the large structural changes that can occur in Pro-Pro sequences on transition from crystals to solution, providing a further example of differences in molecular conformation in the solid state and solution.[37] This study also establishes that appreciable activation barriers can exist for rotation about the C^α–CO (ψ) bond in proline peptides. Finally, spectroscopic evidence suggests that type VI β-turn conformations are populated to a significant extent in Boc-Aib-Pro-Pro-NHMe in solution.

Acknowledgment. This research was supported by a grant from the Indian National Science Academy. B.V.V.P. thanks the Council of Scientific and Industrial Research for the award of a Research Associateship.

Registry No. Boc-Aib-Pro-Pro-NHMe, 84902-97-6.

Supplementary Material Available: Listing of structure factor amplitudes, thermal parameters of non-hydrogen atoms, and positional parameters of hydrogen atom (31 pages). Ordering information is given on any current masthead page.

(36) (a) Chou, P. Y.; Fasman, G. D. *J. Mol. Biol.* **1977**, *115*, 135–175. (b) Iitaka, Y.; Nakamura, H.; Takada, K.; Takita, T. *Acta Crystallogr., Sect. B* **1974**, *B30*, 2817–2825. (c) Vitoux, B.; Aubry, A.; Cung, M. T.; Boussard, G.; Marruad, M. *Int. J. Pept. Protein Res.* **1981**, *17*, 469–479.

(37) Kessler, H.; Zimmerman, G.; Forster, H.; Engel, J.; Oepen, G.; Sheldrick, W. S. *Angew. Chem., Int. Ed. Engl.* **1981**, *20*, 1053–1055.